

ICS-Sniper: A Targeted Blackhole Attack on Encrypted ICS Traffic

Gargi Mitra, Pritam Dash, Yingao Elaine Yao, Aastha Mehta, Karthik Pattabiraman
University of British Columbia
Vancouver, Canada

Email: {gargi, pdash, elainey}@ece.ubc.ca, aasthakm@cs.ubc.ca, karthikp@ece.ubc.ca

Abstract—Operational Technology (OT) networks of industrial control systems (ICS) are increasingly connected to the public Internet, which has prompted ICSes to implement strong security measures (e.g., authentication and encryption) to protect end-to-end control communication. Despite the security measures, we show that an Internet adversary in the path of an ICS’s communication can cause damage to the ICS without infiltrating the ICS. We present ICS-Sniper, a targeted blackhole attack that analyzes the packet metadata (sizes, timing) to identify the packets carrying critical ICS commands or data, and drops the critical packets to disrupt the ICS’s operations. We demonstrate two attacks on an emulation of a Secure Water Treatment (SWaT) plant that can potentially violate the operational safety of the ICS while evading state-of-the-art detection systems.

1. Introduction

Industrial Control Systems (ICS) are networked cyber-physical systems used for automating critical industrial processes, such as manufacturing, water treatment, and power generation and distribution [40]. An ICS consists of two interconnected networks: (i) an Internet-connected Information Technology (IT) network that is used for performing business activities, and (ii) a private Operations Technology (OT) network that connects the critical cyber components and controllers that automate the physical process (i.e., the generation of the plant output). Traditionally, the OT network used to be isolated from the Internet. Security practitioners would thus fortify the IT network, so that it acts as a first line of defense against online threats to the OT network. However, recently OT networks are being directly connected to the Internet to facilitate development and remote monitoring (this is referred to as the Purdue Model 2.0 [17]). Unfortunately, this has again exposed ICSes to rapidly increasing [12, 45, 48] security threats, such as malware and denial of service (DoS) attacks [3, 5, 21, 25, 40, 52]

Restoring a compromised OT network to safe operating conditions is often challenging and expensive for ICS administrators [4]. Thus, ICS administrators have adopted preventative measures to protect OT networks against cyber attacks. These measures are of two types. First, the ICSes employ mechanisms to tolerate some natural network delays and packet losses, which provides a limited degree of

resilience against DoS attacks. Secondly, the administrators have retrofitted security solutions originally designed for IT networks into the OT networks. These include (i) authenticating the endpoint connecting to the OT networks, (ii) encrypting OT messages sent over the Internet, (iii) deploying firewalls and intrusion detection systems (IDS) for preventing and detecting DoS and malware attacks, and (iv) early DoS attack (volumetric) detection techniques [52].

In this work, we present *ICS-Sniper*, a *targeted blackhole attack* on Internet-connected ICS OT networks that works despite the above countermeasures. ICS-Sniper is a new type of DoS attack that aims to compromise two main operational requirements of an ICS – *timeliness* and *synchronization* – and thereby affect ICS performance and safety. The attack drops packets carrying certain strategic data updates and commands for the OT components of an ICS. These include messages that are responsible for changing the action produced by mechanical controllers when certain process variables reach a threshold (e.g., a water pump needs to be turned off when the tank it fills gets full). These messages must be communicated within a specific time to ensure synchronous and safe functioning of all mechanical devices. ICS-Sniper identifies these *critical messages* in the communication path of the ICS on the Internet, and drops the messages to prevent a change in the mechanical action until the ICS incurs damage.

ICS-Sniper differs from prior attacks on ICSes in two ways. First, unlike the attacks that compromise ICS-internal devices [26], ICS-Sniper is executed from a network device *outside of the ICS perimeter*, without compromising any ICS-internal devices, the encryption, or the authentication mechanisms in the OT network. Thus, an adversary can attack an ICS with minimal privileges. Secondly, unlike DoS attacks that flood a network device or drop legitimate packets en masse [3, 21], ICS-Sniper can incur significant damage even by dropping only a *small number of critical* OT network packets that are highly time-sensitive. This makes it challenging for traditional (volumetric) DoS attack detection techniques [31, 55] to detect the attack in real-time.

Identifying the critical messages from a network device outside the ICS perimeter, however, is challenging. This is because the ICS traffic is encrypted. Moreover, ICSes are typically closed, proprietary systems, and an adversary neither has knowledge of its internals nor visibility into its operations and system logs.

ICS-Sniper addresses the above challenge using a novel encrypted traffic analysis (ETA) technique that identifies the critical messages based only on the traffic metadata (e.g., packet lengths, timing). The ETA technique works on the premise that the underlying mechanical actions in an ICS follow a state-transition system, where each state corresponds to a specific action [41] and a transition is invoked by messages exchanged between ICS devices. Furthermore, the messages exchanged by the ICS devices to synchronize the mechanical actions vary across different states [27] and are often time-sensitive. In other words, it assumes that changes in mechanical actions (state transitions) coincide with changes in communication patterns, which are preceded by one or more critical messages.

Based on this premise, ICS-Sniper first constructs a *Labeled Transition System (LTS)* using the metadata of the encrypted OT traffic, which approximates the original state-transition model of the ICS. Specifically, ICS-Sniper mines for periodic patterns in the traffic metadata and maps each pattern to an LTS state. ICS-Sniper identifies the packets transmitted just before the LTS state transitions as critical. Subsequently, ICS-Sniper employs this LTS to predict critical messages in real-time, and drops them. The likelihood of the attack’s success depends on the accuracy of the approximation. Under-approximation might cause it to miss crucial state transitions, whereas over-approximation might lead to dropping of non-critical packets, thereby increasing the chances of getting detected.

We evaluate ICS-Sniper on an in-house testbed that emulates a Secure Water Treatment (SWaT) plant hosted by SUTD [24] and employs encrypted communication, state-of-the-art mechanisms for tolerating network fluctuations, as well as DoS attack detection techniques [19, 31, 55]. We find that ICS-Sniper was able to approximate the state-transition model of the testbed with 100% accuracy. Thereafter, we demonstrate two different attacks on this testbed: (i) a *process delay attack*, and (ii) a *tank overflow attack*. In both cases, ICS-Sniper could identify all the critical messages from the encrypted traffic. In the first attack, the adversary caused a 37.7% reduction in the process output by dropping a set of critical packets for 10 minutes. In the second attack, the adversary caused a water tank to overflow by dropping a different set of critical packets for 10 minutes. Furthermore, we find that *none* of the state-of-the-art DoS attack detection techniques [19, 31, 55] detect the attacks before the ICS was damaged, nor were any of the network delay tolerance techniques able to thwart the attacks.

To the best of our knowledge, *ICS-Sniper is the first targeted blackhole attack on ICS OT networks, which only analyzes encrypted traffic traces from outside the ICS perimeter.*

Contributions summary. We make three contributions.

- (i) We propose a technique for constructing an LTS from the encrypted traffic of the OT network of an ICS, which approximates the state transition model of the ICS (§4).
- (ii) We build a realistic emulation of the SWaT setup at SUTD [24] with network delay tolerance and attack detection mechanisms for evaluating ICS-Sniper (§5).
- (iii) We demonstrate the effectiveness and stealthiness of our

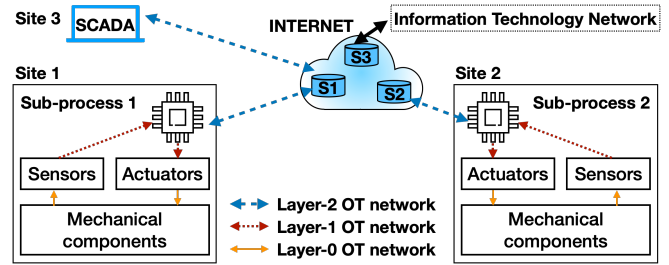


Figure 1: Geo-distributed ICS communication system.

attacks on the emulated SWaT testbed (§6) and propose some countermeasures (§7).

2. Background and Related Work

2.1. Modern ICS Operations

An ICS automates a physical process. Typical ICSes can be broadly categorized into batch processing or continuous processing ICSes. In a batch process, the ICS components process the raw materials in discrete quantities and in a series of steps to produce a final output. Batch processing is often used in manufacturing, food processing, and water treatment plants [10, 22]. The sequence of operations performed by an ICS to process a batch of materials constitute an *operational cycle*. In a continuous process, the ICS components process inputs continuously instead. Examples of such ICSes include power grids. While attacks have been shown on continuous processing ICSes, such as power grids, less attention has been given to batch processing systems. In this work, we largely focus on batch-processing ICSes, which constitute a significant fraction of ICS deployments.

An ICS process consists of sensors that measure various physical parameters, mechanical devices that perform physical actions according to a control logic designed by system architects, mechanical controllers (actuators) that control the devices, and PLCs (programmable logic controllers) that implement the control logic. The control logic ensures that the mechanical devices function in a timely and synchronized manner. For this, the PLCs use the sensor inputs, determine the actions to be taken by the mechanical devices, and transmit the action commands to the mechanical controllers. Other components in the ICS, such as the Human-Machine Interface (HMI) [30], are not directly involved in automated process control, and hence, not relevant to our attack.

In a geo-distributed ICS, a physical process is divided into multiple sub-processes. For instance, chemical dosing and reverse osmosis are two sub-processes of a geo-distributed wastewater treatment process, where water is transported between them using underground pipelines.

Each sub-process may be controlled by one or more PLCs. The PLCs within a sub-process communicate over a local private network. An ICS also has a central Supervisory Control and Data Acquisition unit (SCADA) that communicates with all the sub-processes to supervise them. Figure 1

shows a simplified layout and communication system of a geo-distributed ICS consisting of two sub-processes in two different sites. Unlike traditional ICSes, parts of the OT networks of the sub-processes are connected over the public Internet. The OT communication is implemented using a three-layered architecture. Layer-0 and Layer-1 constitute the *private networks* within a sub-process. Layer-0 connects the sensors to the actuators, while Layer-1 connects the PLCs with the sensors and the actuators within a sub-process. Layer-2, the *plant control network*, connects the PLCs across different sub-processes and the SCADA.

In modern geo-distributed ICSes, the Layer-2 OT networks are directly connected to the public Internet (referred to as the Purdue Model 2.0 [17]). For this, the legacy ICS communication protocols, such as (e.g., Modbus/TCP [7] and CIP/ENIP (Common Industrial Protocol over Ethernet IP) [8]), have been interfaced with the TCP/IP stack of the Internet. Furthermore, industry has adopted TLS (Transport Layer Security) protocol [23] for securing ICS traffic over the Internet [18, 46, 49], to provide confidentiality, integrity, and protection against man-in-the-middle attacks.

2.2. Handling Non-Adversarial Packet Losses

The OT communications may experience delays or drops due to congestion, or variable speeds of the network elements through which the packets pass. ICS designers incorporate two delay tolerance mechanisms. First, to reduce the number of message losses due to fluctuations in network conditions, the OT networks use the TCP protocol [15], which retransmits lost packets until a certain timeout period. Secondly, if some messages are lost or delayed, the sub-process considers the last received message (data updates) as the most recent for its local computations, as shown in existing works [26].

Packet losses may also arise due to failures in an ICS's network devices, sensors, PLCs, or actuators. To mitigate such packet losses, ICSes maintain redundancy in the network devices and other components to take over from the primary devices upon failures. Some ICSes might also have redundant network services purchased from multiple ISPs, which might serve as a backup connection.

2.3. Existing DoS Attacks and Defenses

Existing ICS DoS attack techniques. DoS attacks on ICSes can be classified depending on the adversary's vantage point. (i) *Data modification attacks.* These attacks are executed by adversaries who can infiltrate the ICS networks and gain real-time visibility into the network packet contents [26, 39]. The adversary modifies or drops time-sensitive sensor readings to stall time-critical operations. (ii) *Traffic flow modification attacks.* These are executed by adversaries who cannot infiltrate the ICS network and, therefore, cannot observe the network packet contents to determine their criticality. However, the attacker tries to disable crucial services using one of the following tactics. With *volumetric DoS attacks* [21], it gradually overloads an

ICS service with illegitimate requests to a point where the service cannot process legitimate requests. With *blackhole attacks* [3], on the other hand, it disables a target service by dropping all the traffic sent to it by other services.

Existing DoS detection techniques. The goal of DoS attack detection techniques is to detect the attack in real-time, before they can cause damage to the ICS. There are two broad categories of DoS detection techniques.

(i) *Network traffic-based anomaly detection.* These techniques [16, 31, 55] are used for detecting traffic-flow modification attacks. They work by modeling the ICS traffic flows in the absence of any adversary, and comparing it with the real-time traffic flows of the ICS. These anomaly detection techniques primarily rely on the fact that under a DoS attack, the ICS traffic exhibits a gradual increase (in case of volumetric attacks) or decrease (in case of blackhole attacks) in traffic volume. Because natural network fluctuations also result in a slight increase or decrease in traffic volume from time to time, the challenge for these techniques is to determine the threshold at which the deviation of the traffic volume from normal can be considered malicious. To alleviate this problem, some of these techniques [31] also consider additional factors such as the IP address, port numbers, and protocol-specific field values of the network packets for anomaly detection.

(ii) *Data-driven anomaly detection.* These techniques [19, 39] model the behavior of an ICS by finding correlations between its various sensor readings and process variables in the absence of any adversary. Similar to DoS attack detection techniques, these techniques compare the real-time sensor readings and process variables with the pre-built model to detect possible anomalies at runtime. The challenge for these techniques is to find appropriate thresholds for anomaly detection: high thresholds may lead to missing or delayed detection of attacks before they cause damage to an ICS, whereas low thresholds may lead to false alarms in reaction to natural fluctuations.

2.4. Encrypted Traffic Analysis-based Attacks

ETA has been widely studied in the context of inferring users' website visits [53] and IoT devices [38, 44]. In these scenarios, the adversary profiles the network traffic of a specific website or IoT device by interacting with it as a legitimate user. Subsequently, the adversary observes the traffic of a target user interacting with the website or device, compares the traffic pattern with the profiles it previously recorded, and predicts the content of the interactions.

Unfortunately, the above techniques cannot be directly extended to an ICS environment. This is because, unlike websites and IoT devices, ICS systems do not have a public-facing communication interface. This makes it impossible for an external adversary to interact with ICS components and observe their behavior, as the adversary cannot authenticate with the ICS. Hence, it is challenging for the adversary to build a detailed profile of the ICS. To our knowledge, existing adversarial techniques have focused only on distinguishing encrypted ICS control traffic from other types of

Adversarial Capabilities and Knowledge	PAE	PUE	ENK
1. Knowledge of plant setup and control logic (process documentation)			
(a) System architecture	✓	✗	✗
(b) Control code, msg criticality, process thresholds	✓	✗	✗
(c) Network topology	✓	part	✗
2. Access to ICS-internal devices			
(a) PLCs, Controllers	✗	✗	✗
(b) Network devices	✗	✗	✗
3. Visibility into real-time information			
(a) Live encrypted OT traffic	✓	✓	✓
(b) Traffic decryption key	✗	✗	✗
(c) Live process parameter values	✗	✗	✗
4. Awareness about generic ICS properties			
(a) Periodic & cyclic nature of ICS operations	✓	✓	✗
(b) Correlation between msg frequency & criticality	✓	✓	✗

TABLE 1: Capabilities and knowledge of different adversaries. PAE: Process-Aware External adversary, PUE: Process-Unaware External adversary, ENK: External adversary with no knowledge. We consider a PUE adversary.

traffic on the Internet [9], but not on fine-grained analysis of ICS message criticality using ETA-based techniques.

3. Threat Model and Assumptions

The adversary’s objective is to disrupt the operations of a target ICS, by disrupting the coordination among various devices across different sub-processes.

Adversary position and capabilities. The adversary compromises a network device *outside the ICS perimeter* that carries the traffic between the target ICS components. Many network devices on the Internet have vulnerabilities [29, 35–37, 50] that would grant an adversary root privileges or remote code execution capability on the device. From the compromised device, the adversary can (i) observe unencrypted header fields of all network packets using traffic monitoring tools, e.g., tshark [54], and (ii) drop packets.

The adversary cannot compromise the ICS-internal devices. Therefore, it cannot access device logs, nor observe the mechanical devices. The adversary cannot hijack the decryption key or break the encryption of the ICS traffic.

We assume that the adversary can compromise a router that routes the target ICS’ traffic, and identify the target flows using known techniques [9]. We focus on demonstrating how the adversary can identify critical messages within the ICS flows and drop them strategically.

Adversary’s background knowledge of the ICS. We consider a *process-unaware* external (PUE) adversary that is both common and realistic. The adversary has *no knowledge about the system design, control algorithm, or the implementation details* of the target ICS. However, the adversary is *aware of the general properties of ICS systems*, e.g., the repetitive and periodic nature of ICS operations, and the fact that ICS sub-processes can perform a fixed set of actions.

For comparison, we also consider two additional external adversaries on the two extreme ends of the spectrum [52]. First, we consider a process-aware external (PAE) adversary who has access to the operational manual of the target ICS. The operational manual is usually distributed only to trusted

employees and the OT device vendors. This adversarial model covers adversaries with unauthorized access to the manual, and ex-employees who turn rogue and exploit their knowledge of the process details to attack the ICS. Such attacks have been carried out on water treatment plants in the wild [1, 51]. However, these adversaries do *NOT* have access to system passwords and traffic decryption keys. Second, we consider an external adversary with no general knowledge about ICSES (ENK), which can only perform a volumetric DoS attack. Table 1 provides a comparison of the capabilities and knowledge about the target ICS available to the four adversary models. The PUE adversary has intermediate levels of capabilities and knowledge about the target ICS. Table 1 shows the capabilities of the PUE model in comparison with the two additional external adversarial models each on the opposite ends of the spectrum [52].

4. ICS-Sniper

In this section, we first describe an ICS as a state-transition system. We then give a high-level overview of ICS-Sniper and describe its two phases.

4.1. ICS as a State Transition System

Over a complete operational cycle of a typical ICS, each sub-process follows a state-transition model. Each state in this model corresponds to a certain operational state of its mechanical devices. A state transition represents a change in the state of one or more mechanical devices. Furthermore, a sub-process might have a different network communication pattern in each state. ICS-Sniper relies on these characteristic features of ICSES. In this section, we describe this concept in detail with an example.

ICS example. Consider a simple ICS consisting of two sub-processes p_1 and p_2 , which are located in two different geolocations. The sub-process p_1 contains two mechanical devices d_{11} and d_{12} , two sensors $sensor_1$ and $sensor_2$, and a PLC plc_1 . The sub-process p_2 contains devices d_{21} and d_{22} and a PLC plc_2 . Each of the four devices can either be turned ON or OFF, and they must operate in a coordinated manner to meet the process quality and safety standards. The sensors in p_1 measure different physical parameters local to p_1 and, accordingly, take a value of HIGH or LOW each. The sensor values determine the states of the devices in p_1 , which in turn, determine the states of the devices in p_2 . The PLC in each sub-process reads inputs from sensors (if any), runs the logic controlling the changes in the state of the devices in the sub-process, and sends network traffic to other sub-processes for coordination between the sub-processes.

Figure 2 shows a snippet of the control logic code, P1_Control and P2_Control, which govern the sub-processes p_1 and p_2 , respectively. At the beginning of the operational cycle, all four devices are in OFF state (lines 4-5 of both algorithms) and both the sensors in p_1 have a LOW value. The sensor values change to HIGH due to certain physical events. When $sensor_1$ value turns HIGH, device d_{11} turns ON. When $sensor_2$ value turns HIGH while d_{11} is

```

1 PROGRAM P1_Control
2 //Initializing devices
3 VAR
4     d11Status: BOOL := False; // d_11 is OFF
5     d12Status: BOOL := False; // d_12 is OFF
6     sensor1val: INT := 0;
7     // sensor_1 = LOW
8     sensor2val: INT := 0;
9     // sensor_2 = LOW
10 END_VAR
11 // Main block
12 IF sensor1val==1 AND NOT d11Status THEN
13     d11Status := TRUE; // Turn d_11 ON
14     IF sensor2val==1 AND NOT d12Status THEN
15         d12Status := TRUE; // Turn d_12 ON
16     END_IF
17 END_IF
18 ...
19 // End of P1_Control

1 PROGRAM P2_Control
2 //Initializing devices
3 VAR
4     d21Status: BOOL := False; // d_21 is OFF
5     d22Status: BOOL := False; // d_22 is OFF
6 END_VAR
7 // Main block
8 IF NOT d21Status AND d11Status THEN
9     d21Status := TRUE; // Turn d_21 ON
10     IF NOT d22Status AND d12Status THEN
11         d22Status := TRUE; // Turn d_22 ON
12     END_IF
13 END_IF
14 ...
15 // End of P2_Control

```

Figure 2: Control algorithms for a sample ICS.

ON, device d_{12} also turns ON (lines 12-17 of P1_Control). Unlike the devices in p_1 , devices in p_2 are turned ON by *remote events*, i.e., events occurring in p_1 . Device d_{21} is turned ON when device d_{11} in p_1 turns ON (lines 9-10 of P2_Control). Device d_{22} turns ON if d_{12} (in p_1) turns ON while d_{21} is also ON (lines 11-12 of P2_Control).

The above control logic are executed on PLCs, plc_1 and plc_2 , respectively. In this example, plc_1 reads values of $sensor_1$ and $sensor_2$ over its local private network and determines the states of its devices d_{11} and d_{12} . In contrast, plc_2 requests parameters pertaining to the remote sub-process p_1 and determines the states of the devices in d_{21} and d_{22} . For this, plc_2 continuously sends requests to plc_1 for the status of the devices in p_1 , and plc_1 responds to these requests. This communication is over the Internet.

State-transition system. Figure 3 shows the state-transition diagram of p_1 and p_2 , along with the messages exchanged between them in each state. At the beginning of the operational cycle of the ICS, p_1 and p_2 are in states S_{11} and S_{21} respectively, where all their devices are turned OFF. While in state S_{21} , p_2 keeps requesting p_1 for the state of d_{11} (message m_1), and p_1 keeps responding to these requests

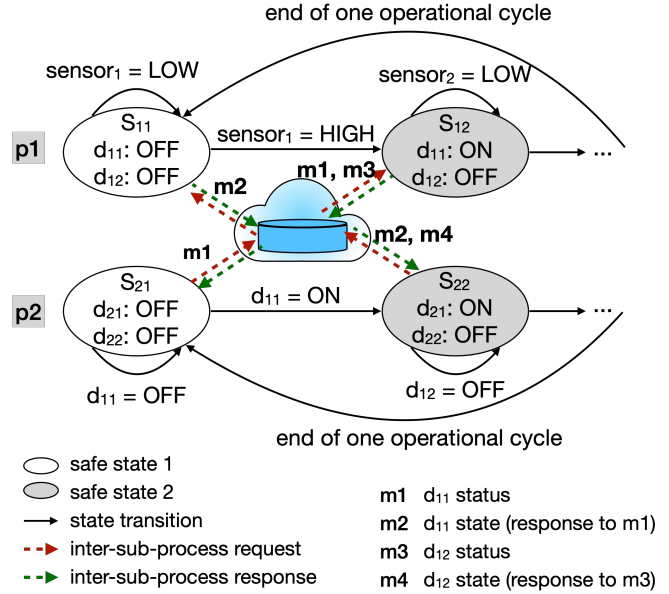


Figure 3: ICS operations and communication of the sample ICS (described in §4.1) as a state-transition system

(message m_2). This is necessary for p_2 to determine when to turn device d_{21} ON (line 9 of P2_Control in Figure 2). The two sub-processes repeat this request/response pattern of communication until $sensor_1$ turns HIGH and d_{11} turns ON. Thereafter, p_1 transitions to a new state S_{12} , and responds with ‘d11Status=TRUE’ when p_2 requests for the state of d_{11} . Consequently device d_{21} in p_2 turns ON, and this causes p_2 to transition to a new state S_{22} . In this new state, p_2 needs to determine when to turn d_{22} ON (lines 11-12 of P2_Control). To do so, it starts requesting p_1 for the status of d_{12} , and p_1 keeps responding to its requests, resulting in two extra messages, m_3 and m_4 between them.

State changes triggered by remote events (as seen in p_2) cannot occur instantaneously, since the inter-sub-process communications might incur some communication delay on the Internet path. While the system designer implements delay tolerance mechanisms to account for benign communication delays, the tolerance is limited by a threshold value (say, δ_t). If a scheduled state transition is delayed beyond δ_t , the devices of the two sub-processes would lose their coordination, and the performance and safety of the ICS would be jeopardized. For instance, assume d_{11} is a pump that sends water to a tank in p_2 through a pipeline, and d_{21} is the water inlet valve that allows water into the tank. If d_{21} does not turn ON within a certain time of d_{11} getting turned ON (state transition delayed in p_2), it might result in an unacceptably high pressure on the pipe and damage it.

4.2. ICS-Sniper: An Overview

At a high level, the goal of ICS-Sniper is to disrupt the coordination among the sub-processes and create unsafe operating conditions. For this, the adversary must identify the

messages critical for the coordination and drop them or delay them beyond the tolerable delay thresholds. Thus, ICS-Sniper works in two phases. In the *Sub-process Profiling Phase*, it first identifies the critical messages. Subsequently, in the *Active Phase*, it observes the live sub-process traffic and drops the critical messages at appropriate times.

A key challenge for the adversary in both phases is to identify the critical messages from the encrypted traffic. We start by discussing four key observations that enable the adversary to overcome this challenge.

O1. Messages that trigger state transitions are more time-sensitive than others. Unusual delays in communicating these messages (e.g., beyond δ_t) may lead to a loss of coordination among the sub-processes, thereby resulting in an unsafe operating condition for the ICS. Henceforth, we refer to these messages as *critical messages*.

O2. The messages between sub-processes are sent via ICS communication protocols, such as CIP/ENIP over TLS and secure Modbus-TCP. The messages are typically small and these protocols encrypt each message and encapsulate it into a single TCP packet before transmitting it over the Internet [2, 42]. Thus, the length of the TCP packets reveals the length of encapsulated messages.

O3. A state transition in a sub-process causes a shift in its communication patterns. In the example of §4.1, p_1 and p_2 keep repeating the message sequence (m_1, m_2) while they are in state S_{11} and S_{21} , respectively. However, after p_1 transitions to S_{12} and p_2 transitions to S_{22} , they start repeating a different sequence (m_1, m_2, m_3, m_4) . Thus, a shift in the communication pattern of a sub-process indicates the presence of one or more critical messages in the final repetition of the previous message sequence.

O4. A state transition of a sub-process might be triggered by one or more messages from a remote sub-process. The control logic may require all the messages (i.e., an AND), or only one of the messages (i.e., an OR), or a subset of the messages determined by a more complex combination. Thus, there might be more than one critical message in the last round of message repetition.

Thus, ICS-Sniper detects repetitions and shifts in communication patterns from packet metadata, such as packet length, direction, and inter-packet timings, and designates all the packets in the last repetition round of each pattern as critical. We elaborate on the two attack phases.

4.3. Sub-process Profiling Phase

In this phase, ICS-Sniper models the communications of the target sub-process over a complete operational cycle, using traffic metadata, to recover its original state-transition model. For simplicity, we consider a scenario where ICS-Sniper targets a single sub-process in the ICS. ICS-Sniper profiles the target sub-process using four steps.

Step 1: Capture the network traffic for a complete operational cycle of the target sub-process. ICS-Sniper needs to determine the start and end points of an operational cycle and capture *all the packets* corresponding to a complete operational cycle of the target sub-process. Missing

Packets	pkt_1	pkt_2	pkt_3	...	pkt_n
Length	l_1	l_2	l_3	...	l_k
Source IP	x.x.x.x	y.y.y.y	x.x.x.x	...	y.y.y.y
Destination IP	y.y.y.y	x.x.x.x	z.z.z.z	...	x.x.x.x
Metadata ID	1	2	3	...	100

TABLE 2: An example of packet metadata captured by ICS-Sniper in Steps 1 and 2 of profiling.

packets or extra packets from the previous or next cycles might result in an inaccurate communication model. We describe the challenges and how ICS-Sniper addresses them to precisely a complete operational cycle’s packets.

Challenge (C1): Identifying the first and last packets of an operational cycle from the network traffic. Lack of access to the operational manual and message contents makes it challenging for ICS-Sniper to identify the first and last packets corresponding to an operational cycle when it eavesdrops on the traffic of the target sub-process.

Addressing C1. ICS-Sniper leverages a specific characteristic of the batch-processing ICSes. Such an ICS typically performs a sequence of operations on a batch of inputs, remains idle for a specific amount of time while the next batch of inputs is loaded onto the mechanical system for processing, and repeats the same sequence of operations on the next batch. The sub-processes have a high network activity during the operational phase of the ICS, while there is negligible or no network activity during the idle phase. Thus, the inter-packet timings of a sub-process are far lower during the operational phase than the idle phase.

ICS-Sniper identifies the first and last packets of the operational cycle of the target sub-process by observing the inter-packet timings. ICS-Sniper starts to capture the network traffic at a random instant of time and computes the inter-packet timings. At this point, there can be two possible scenarios. **(1)** The sub-process is in the middle of an operational phase. ICS-Sniper keeps computing the inter-packet timings, and when it observes an interval much greater than the average timing observed so far, it infers that the current operational phase has ended and a new one has started. ICS-Sniper then considers the latest packet as the first packet of the next operational cycle and discards all other packets. It repeats this process until it again observes a period of inactivity greater than the average timing. **(2)** The sub-process is in the middle of an idle phase. ICS-Sniper observes a period of inactivity followed by a stream of packets with low inter-packet timings. In this case, ICS-Sniper keeps capturing packets until there is a period of inactivity much greater than the average inter-packet time.

Challenge (C2): Packet loss due to natural network fluctuations. When ICS-Sniper captures the network traffic for a complete operational cycle of the target sub-process, a few packets may be lost and retransmitted several times due to natural network fluctuations.

Addressing C2. ICS-Sniper captures the packet sequence in an operational cycle, removes retransmitted packets using TCP sequence numbers, and records the sequence of unique packets. To ensure that all the packets for a complete oper-

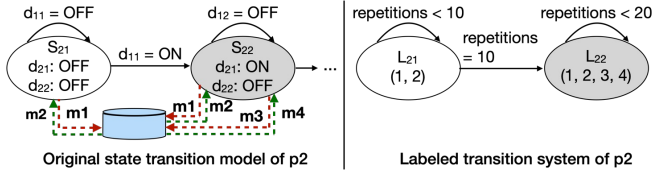


Figure 4: A scenario where the LTS of p_2 (of sample ICS in §4.1) constructed by ICS-Sniper aligns perfectly with its original state transition model. The metadata identifiers for m_1, m_2, m_3 and m_4 are 1, 2, 3 and 4 respectively. In state S_{21} , p_2 repeats the sequence (m_1, m_2) 10 times and in S_{22} , it repeats the sequence (m_1, m_2, m_3, m_4) 20 times.

ational cycle of the target sub-process have been captured, ICS-Sniper repeats this step until it observes a consistent sequence of packets for every operational cycle of the sub-process. ICS-Sniper selects one of the consistent packet sequences for further processing.

Step 2: Extract the metadata of captured packets. In this step, ICS-Sniper extracts the metadata of the encrypted packet sequence captured in Step 1. Specifically, for each packet, it records the length and the source and destination IP addresses of the packet. To simplify subsequent processing, ICS-Sniper assigns a unique metadata identifier to each unique tuple of (packet length, source IP, destination IP). The output of this step is a sequence of metadata identifiers. Table 2 shows an instance of the packets captured in Step 1, their metadata, and the identifiers assigned by ICS-Sniper to each unique metadata tuple. In this case, the output of Step 2 is $\{1, 2, 3, \dots, 100\}$.

Step 3: Mine for patterns indicating state transitions. Next, ICS-Sniper mines the metadata sequence extracted in Step 2 to find all sets of shortest length sub-sequences that have at least two consecutive occurrences¹. For our attack, we only mine the packet sequences based on packet lengths and ignore the packet timings. A future attack may further leverage packet timings for higher accuracy.

We adapt a known technique [20] that has been used for mining cyclic and periodic patterns in ICS sensor values. Specifically, we make two modifications to the original algorithm to capture the characteristics of ICS traffic. First, unlike the original algorithm, which accounts for noise in the sensor values, our algorithm does not need to account for any noise in the metadata sequence. This is because the ICS communication protocols encode the values from a given sensor into fixed-length payloads and encapsulate them into packets with fixed-length headers. This simplifies the original algorithm. Secondly, because ICS communications follow a request-response pattern, we incorporate a constraint that the lengths of the patterns in the metadata sequence are always multiples of two, and that there are no residual elements in the sequence after extracting all the elements.

1. Our mining algorithm relies on the assumption that there are at least two consecutive occurrences of each message sequence because we have observed empirically that the operations in each state of a sub-process are repeated at least once. Handling non-repeating sequences is trivial.

Algorithm 1 in Appendix A shows the metadata pattern mining technique. ICS-Sniper scans the metadata sequence from the first element onwards, and identifies the constituent shortest sub-sequences that occur at least twice consecutively. Once it finds a repeating sub-sequence, ICS-Sniper records it as a pattern, and also records the number of times it repeats. When ICS-Sniper reaches a point in the sequence where the pattern does not repeat any more, it assumes that it has detected a state transition. It then truncates the sequence at that point, and repeats the above process over the rest of the sequence. However, ICS-Sniper might encounter a scenario where there is no repetitive sub-sequence in the truncated sequence (i.e., the sequence has residual elements after the extraction of repeating patterns). This indicates that one or more of the preceding patterns are part of a longer pattern. In this case, ICS-Sniper rescinds the last recorded pattern (say, of length x), adds it back to the beginning of the truncated sequence, and begins to search for a new pattern, starting with a length of $(x+2)$. ICS-Sniper keeps repeating the above steps until it splits the entire metadata sequence into a set of repetitive patterns, where each pattern has an even length and has at least two consecutive occurrences.

As an example, if the input sequence to the algorithm is $\{1, 2, 1, 2, 1, 2, 1, 2, 3, 4, 1, 2, 1, 2, 3, 4, 5, 6, 1, 2, 1, 2, 1, 2, 3, 4, 1, 2, 1, 2, 3, 4, 5, 6\}$, the output would be $patterns = \{(1, 2), (1, 2, 1, 2, 3, 4, 1, 2, 1, 2, 3, 4, 5, 6)\}$ and $repetitions = \{2, 2\}$. Note that, the extracted patterns are stored in the order of their occurrence in the input sequence.

Step 4: Construct a Labeled Transition System (LTS). Finally, ICS-Sniper constructs a LTS from the patterns extracted in Step 3. Each pattern corresponds to one LTS state. A transition from a state L_i to the next state L_j occurs when the number of repetitions of the pattern corresponding to L_i reaches its repetition count as recorded in Step 3.

The constructed LTS will ideally match the state transition model of the ICS. Figure 4 shows the example of an ideal LTS constructed by ICS-Sniper for the sub-process p_2 shown in Figure 3. In practice, the LTS construction technique faces two fundamental challenges, where it either (1) generates incorrect extra states (overapproximates the original system), or (2) misses state transitions (underapproximates the original system). We discuss these scenarios.

Scenario 1: Overapproximation occurs when the number of states in the LTS is higher than the number of states in the original state transition model. This happens when the original metadata pattern of any of the states is composed of smaller repetitive patterns. For instance, consider a sub-process whose original patterns are $\{(1, 2), (3, 4, 3, 4, 5, 6, 5, 6, 3, 4, 3, 4, 5, 6, 5, 6)\}$. In this case, the output of Algorithm 1 would be $\{(1, 2), (3, 4), (5, 6), (3, 4), (5, 6)\}$. First, ICS-Sniper constructs an LTS with 5 states based on this output. However, this overapproximation would lead to false positives, i.e., ICS-Sniper would predict a state transition when there is none. If this happens, ICS-Sniper might end up attacking the ICS at the wrong time, and get detected before causing any damage to the ICS.

To mitigate this issue, ICS-Sniper checks the extracted pattern set for potentially mergeable patterns, and constructs

additional candidate LTSes by merging the smaller patterns. Specifically, it creates LTSes for all possible merges of two or more patterns. For the given example, ICS-Sniper would construct one additional candidate LTS with the pattern set $\{(1, 2), (3, 4, 3, 4, 5, 6, 5, 6, 3, 4, 3, 4, 5, 6, 5, 6)\}$.

Once ICS-Sniper does not find any mergeable patterns, it proceeds to construct an LTS with the patterns extracted.

Scenario 2: Underapproximation occurs when the number of states in the LTS is lower than the number of states in the original state transition model of the target sub-process. This happens when adjacent states have the same metadata pattern, or the pattern of one state is a multiple of that of the adjacent state. ICS-Sniper builds only one LTS state for such patterns. For instance, in the example shown in Figure 3, let the metadata identifiers of m_1, m_2, m_3 and m_4 be 1, 2, 1 and 2 respectively (i.e., m_1 and m_3 have the same length and direction, and m_2 and m_4 have the same length and direction). In this case, the ideal LTS would comprise two states – one for the pattern (1, 2) (to be aligned with S_{21}), and another one for the pattern (1, 2, 1, 2) (to be aligned with S_{22}). Instead, ICS-Sniper would construct only one LTS state for the pattern (1, 2). Hence, ICS-Sniper would not be able to identify the transition from S_{21} to S_{22} from the network traffic patterns. Moreover, dropping packets in the last repetition round of the solitary pattern (1, 2) might not cause any impact on the plant if the last two packets of the original pattern (1, 2, 1, 2) are not critical.

This is a fundamental limitation and may affect the efficacy and detectability of ICS-Sniper. However, consecutive states having similar metadata patterns—leading to underapproximation—are uncommon in ICSes. Indeed, ICS-Sniper did not suffer from underapproximation errors while constructing the LTS for our SWaT case study (see §6.1)

4.4. Active Attack Phase

Once ICS-Sniper has profiled the target sub-process, it proceeds to drop the critical packets in real-time. It begins to observe the traffic and waits till it identifies the beginning of a new operational cycle. For identifying the first packet of an operational cycle, ICS-Sniper employs the technique used in the first step of the profiling phase. For identifying critical packets, ICS-Sniper refers to the LTS constructed in Step 4 of the profiling phase. ICS-Sniper starts with the first LTS pattern and matches the metadata of the real-time traffic with it to count the number of repetitions that occurred. As soon as it observes the penultimate repetition of the pattern, it activates a packet drop routine to drop all the packets in the final round of repetition of the pattern.

As per our adversary model, ICS-Sniper has no knowledge of the threshold delay of the critical messages, nor the damage that might be caused by dropping them. Therefore, ICS-Sniper drops the packets for an arbitrary amount of time and then checks if it has impacted the sub-process. ICS-Sniper cannot assess the real damage caused by the attack from outside the ICS perimeter. Instead, it attempts to understand if the attack has deviated the sub-process from its ideal behavior. For that, it observes the traffic metadata till

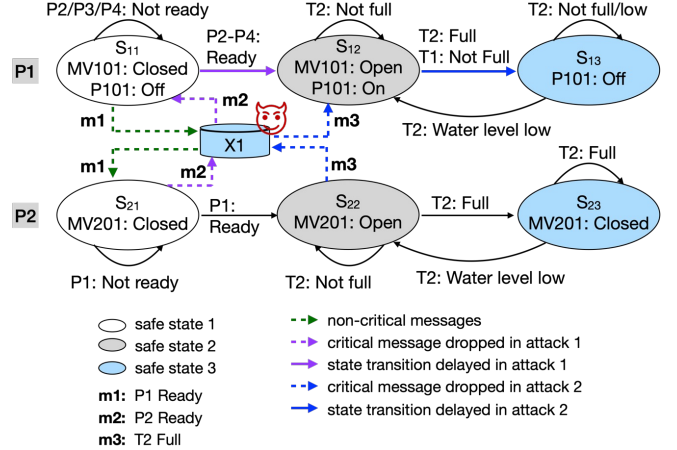


Figure 5: Original state-transition model of P1 and P2 of the SWaT testbed (§5), and adversarial goals. Dropping message m_2 would prevent the transition $S_{11} \rightarrow S_{12}$, while dropping m_3 would prevent $S_{12} \rightarrow S_{13}$ in P1.

the end of the operational cycle. If at any point the observed metadata does not match the stored LTS, ICS-Sniper infers that the sub-process has been negatively impacted. However, a deviation in behavior might also indicate corrective actions performed by the sub-process in response to the attack. In reality, while a corrective action might prevent extreme damage (e.g., poisoning of treated water), additional actions performed during an operational cycle might have a negative impact such as low process throughput.

Note that ICS-Sniper can be configured to target any state transition of the LTS. If there is more than one candidate LTS, ICS-Sniper begins with the one that has the least number of states to reduce false positives and detectability.

5. Experimental Setup

We describe our ICS testbed, the emulated Secure Water Treatment (SWaT) plant setup on the testbed for evaluating ICS-Sniper, and the implementation of the attacks in the setup. We also describe the attack detection techniques that we later use to evaluate ICS-Sniper efficacy.

5.1. SWaT plant

Figure 9 in Appendix B shows the architecture of the complete SWaT plant hosted at SUTD [24]. The plant purifies wastewater in six stages, each controlled by a sub-process: raw water storage ($P1$), chemical dosing ($P2$), ultrafiltration ($P3$), dechlorination ($P4$), reverse osmosis ($P5$), and backwash ($P6$).

For our attack, we focus on two specific sub-processes of the plant as shown in Figure 10. Sub-process $P1$ collects raw wastewater in Tank T1 and pumps it out to the sub-process $P2$ for chemical dosing. $P1$ and $P2$ have a tank each, namely, T1 and T2 respectively. Each tank is fitted with a water level sensor, a water inlet valve (MV101 for

T1 and MV201 for T2) that fills water into the tank when open, and a pump (P101 for T1 and P201 for T2) that draws water out of the tank to fill the tank in the next sub-process when turned on. The water inlet valves and pumps are controlled by the respective PLCs. The maximum water level height in T1 that keeps the plant functional is 800 cm. Water levels beyond 900 cm and 1000 cm are considered risky and damaging, respectively.

All the sub-processes start in an idle state at the beginning of an operational cycle. Being the first sub-process, $P1$ is the last one to get activated. $P1$ opens its water inlet valve MV101 and turns on the pump P101 only after it receives messages from processes $P2$ – $P4$, indicating they are ready to start operations.

Figure 5 shows the the state transition model of the sub-processes $P1$ and $P2$. We built this model based on the open-source simulation of the process [13] and publicly available details about the SWaT testbed [24]. In addition to the critical messages, $P1$ and $P2$ exchange 10, 14, and 15 other messages repetitively when $P1$ is in state S_{11} , S_{12} , and S_{13} respectively. These messages are not critical and do not trigger a state transition.

5.2. Testbed

As we did not have access to the real ICS, we implemented and evaluated our attacks on a testbed that we developed to mimic real industrial processes, i.e., execute the control logic of real industrial processes and emulate the Layer-2 network communications. We describe the testbed and the emulation of the SWaT plant on the testbed.

The testbed uses MiniCPS [6], a popular framework for emulating distributed industrial control systems and their network communications. The MiniCPS framework is a network of Virtual Machines (VMs), where each VM runs the control logic of a real PLC, and the physical process is simulated using mathematical models. MiniCPS is built on top of Mininet [34], a well-known network emulator. The network topology between the VMs mimics that of the original plant. The OT communication protocol between the VMs is emulated by well-known Python libraries [6, 28]. Currently, the testbed supports two popular OT communication protocols: (i) the CIP/ENIP [8], and (ii) the Modbus/TCP [7]. Furthermore, we assume that the traffic between each pair of VMs is encrypted using TLS [46, 49]. However, since the Python libraries do not use TLS encryption, we augment them with a packet-size translator that converts the lengths of plaintext messages to their corresponding ciphertext lengths if they would be encrypted using TLS. Thus, we only use the packet length information from the TLS metadata in our experiments. This is a reasonable setup since a real adversary cannot access the encrypted packet contents as per our threat model (§3).

We implement the state-of-the-art network delay tolerance mechanism (§2.2) in the testbed. If a message to a sub-process is dropped or delayed beyond a pre-configured timeout period, the target sub-process reuses the data from the last received version of the message.

The testbed provides three benefits. **(1)** The configurability of communication protocols and encryption techniques allows the emulation of a wide range of ICS OT networks. **(2)** The use of a network emulator allows researchers to transmit the messages over the network stack and observe the OT network characteristics without having to connect the testbed to the Internet. This is particularly useful for testing various attacks in a sandboxed environment. **(3)** Since VMs are portable, the testbed can be easily shared.

Emulated SWaT. We emulated the SWaT plant (§5.1) on the testbed and refer to it as the SWaT testbed. The testbed consists of six Programmable Logic Controllers (PLCs), one for each of the six sub-processes, and a SCADA unit. The PLCs and SCADA are implemented in seven virtual machines (VMs), each connected to a Mininet switch that emulates an Internet router. These switches are connected in a mesh topology emulating the Internet. The control logic of the setup is adapted from an open-source Python simulation of the SWaT testbed [13], where we replaced the process-level PLC communications with network-level inter-VM communications. We configure the testbed to use the ENIP protocol and generate similar traffic as the original plant [24] by using the same message syntax, semantics, and frequency of communications.

5.3. Attack Execution

We consider an adversary whose objective is to cause disruptions in communications between sub-processes $P1$ and $P2$. We place ICS-Sniper on the switch X1 (Figure 5) to emulate an adversary who compromises a network device on the communication path connecting $P1$ with the other sub-processes. ICS-Sniper relies on three components: **(i)** a packet capturing tool (we use tshark [54]), **(ii)** an LTS construction module implemented in Python by us, and **(iii)** a network controller for dropping packets (we use *ovs-ofctl* [43] to implement traffic rules for dropping packets).

5.4. DoS Detection Techniques

To the best of our knowledge, there is no technique for effectively detecting targeted blackhole attacks on ICS OT traffic. Existing ICS DoS attack detection techniques [16, 19, 31, 39, 55] (discussed in §2.3) were designed either for detecting volumetric DoS attacks from network traffic, or for identifying anomalous sensor readings. Nevertheless, we evaluate if these techniques can detect the attacks executed by ICS-Sniper. For our evaluation, we use the following three state-of-the-art attack detection techniques, each of which represents a broad category of attack detectors.

Statistical Similarity-based Traffic Anomaly Detector (NND) [55]: This technique relies on the premise that the OT traffic consists of repetitive periodic patterns. It first learns the patterns of transmitted and received packet counts between device pairs over time. Next, in real-time, it employs a sliding window over the network traffic and computes the packet counts in each observed window. It compares the observed packet counts with the learned patterns using the

nearest nearest-neighbor distance measure and detects potential anomalies (e.g., unusually high/low traffic volume).

Probabilistic Automata-based Traffic Anomaly Detector (Detano) [31]: Detano is a protocol-aware traffic anomaly detector, which learns traffic patterns from packet counts as well as protocol-specific packet headers. It identifies packets with unusual protocol headers and unusual volumes of packets of one or more protocols (e.g., a high number of retransmissions or volumetric DoS attack traffic). Similar to NND, it uses a sliding window method for selecting and comparing network traffic segments with learned patterns to detect DoS attacks at early stages.

Process Invariant-based Anomaly Detector (PAD) [19]: PAD uses ML algorithms to mine process invariants from past system logs. Each system log entry contains the readings collected from sensors and values of process variables, which are logged by the process at periodic intervals. PAD processes the log entries generated over a long time period under non-adversarial conditions. It identifies a set of logical assertions that hold true for the process at any instant of time under non-adversarial conditions. For instance, an invariant mined by PAD for the SWaT system described in §5.2 is ‘ $MV101.Status = Open \rightarrow P2.State \neq S_{21}$ ’. PAD detects anomalies in real-time by periodically checking if the sensor readings and process variables violate any invariant.

6. Evaluation

We answer three questions in our evaluation. **(1)** Can ICS-Sniper generate an accurate communication profile of the SWaT testbed and identify critical messages to drop? (§6.1) **(2)** What is the impact of ICS-Sniper’s attack on the SWaT testbed? (§6.2) **(3)** How well can the state-of-the-art attack detection techniques detect ICS-Sniper? (§6.3)

6.1. Profiling Accuracy

The success of ICS-Sniper during the active attack phase depends on how accurately it was able to profile the target sub-process beforehand. We determine the profiling accuracy by measuring **(i)** how closely the LTS constructed during profiling represents the original state transition model of the system, and **(ii)** the recall and precision with which ICS-Sniper identifies the critical messages.

Experiment. We ran the SWaT emulation for three complete operational cycles of $P1$ (8 hours of operation per cycle). To mimic natural network fluctuations, we induced brief (30-60s) periods of packet drops and delays at random intervals during one of three operational cycles. To profile $P1$, ICS-Sniper captured its metadata sequence at $X1$.

Ground Truth. The original state transition system of $P1$ has three states (Figure 5). In one complete operational cycle, $P1$ repeats a sequence of 26 messages 3 times consecutively in state S_{11} , 30 messages 125 times in state S_{12} , and 32 messages for 15226 times in state S_{13} . In the final repetitions of each state, 6, 2, and 2 messages are critical, respectively.

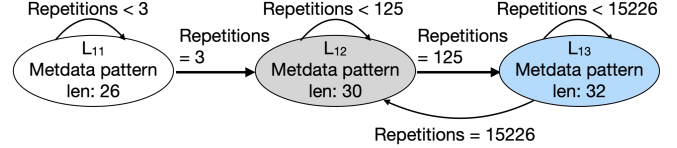


Figure 6: LTS of $P1$ of the SWaT testbed (§5), as constructed by ICS-Sniper.

Accuracy of the LTS. The LTS of a sub-process is an accurate representation of its original state transition system if (a) the number of states in the LTS is equal to that in the state transition system, and (b) the metadata of the messages exchanged in each state of the original system are grouped within the corresponding LTS state.

To construct the LTS, ICS-Sniper first splits the input metadata sequence into that of individual operational cycles by examining inter-packet timings. While the inter-packet timings during the operational phase of the SWaT plant were in the order of milliseconds, the time between the last packet and the first packet of consecutive cycles was two hours.

On analyzing the metadata sequence of the operational cycle using Algorithm 1, ICS-Sniper detected three patterns in the metadata sequence, each of which had the same number of repetitions as those of the message sequences in the corresponding state of the original state transition system. Figure 6 shows the LTS of $P1$ constructed by ICS-Sniper. The LTS matched the ground truth state transition system because, by design, the metadata sequence of adjacent states of $P1$ were distinct (thus, causing no under-approximation), and the metadata sequence of no state had cyclic repeating sequences within itself (thus, causing no over-approximation).

Recall and precision for critical messages. ICS-Sniper should ideally drop *all the critical messages* that trigger a target state transition, i.e., the recall of critical messages must be 100%. For each attack, we compute the recall over an operational cycle as $\frac{\text{No. of critical messages dropped}}{\text{Actual no. of critical messages}} \times 100\%$.

Similarly, ICS-Sniper should drop only the critical messages and not the other messages (i.e., achieve a high precision) so that it does not trigger any DoS attack detection technique. For each attack, we compute the precision over an operational cycle as: $\frac{\text{No. of critical messages dropped}}{\text{Total no. of messages dropped}} \times 100\%$.

Because ICS-Sniper was able to capture the original traffic patterns of the SWaT testbed in the LTS with 100% accuracy, the recall value for the critical messages was also 100%. This is because once ICS-Sniper detects a repetitive pattern, it considers all the packets in its last round of repetition as critical and drops them. Therefore, it does not miss any critical packet.

While ICS-Sniper drops all packets in the last round of repetition of each pattern, not all of them are actually critical. Therefore, for the transition $S_{11} \rightarrow S_{12}$, the precision of ICS-Sniper was 23%, while for the transition $S_{12} \rightarrow S_{13}$, its precision was 6.7%. While the precision is on the low side despite the targeted nature of our attack, it is much higher than that for a conventional DoS attack. For instance, if a

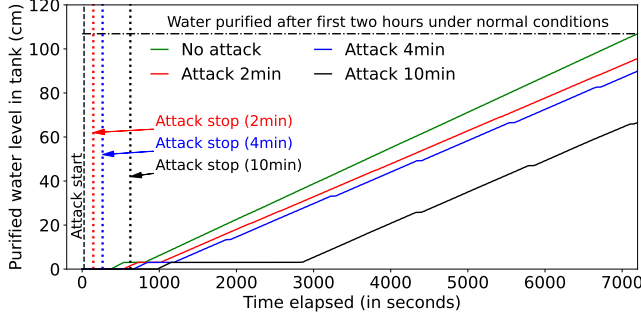


Figure 7: Impact of Process Delay Attack on the testbed.

conventional DoS attack ends up dropping k repetitions of the messages in S_{11} for delaying the transition $S_{11} \rightarrow S_{12}$, its precision would be $\frac{1}{k} \times$ that of ICS-Sniper’s.

6.2. Attack Impact

Experiment. As mentioned earlier, ICS-Sniper is agnostic of the implications of the state transitions and the impact of delayed transitions on the sub-process. Rather, it drops packets whenever it predicts an upcoming state transition during the active attack phase. Hence, we study the impact of two attacks on the SWaT testbed: one in which it delays the transition $L_{11} \rightarrow L_{12}$, and another in which it delays the transition $L_{12} \rightarrow L_{13}$ (Figure 6). For simplicity, we refer to these attacks as *Process Delay Attack* and *Tank Overflow Attack*, respectively, based on the effect that the attacks are expected to have on the sub-process. We did not include the transition $L_{13} \rightarrow L_{12}$ in our experiments, as delaying this transition would have a similar impact on $P1$ as delaying the transition $L_{11} \rightarrow L_{12}$.

The operational cycle of the SWaT testbed is 8 hours. Under non-adversarial circumstances, both state transitions take place within the first hour of the operational cycle. Therefore, we run the SWaT process only for the first two hours of its operational cycle and execute the active attack phase of ICS-Sniper within that time frame.

To understand the effects of an attack, we execute only one attack in each operational cycle, i.e., ICS-Sniper delays only one state transition per cycle. We assess the impact of the attacks on the SWaT testbed by inspecting if an attack has caused $P1$ to deviate from its normal operating behavior. Specifically, we look for either a reduction in process throughput or a violation of the safety constraints.

Process Delay Attack. In this attack, ICS-Sniper successfully dropped all the 26 packets of L_{11} during their third repetition. We execute this attack for three different packet drop durations (2, 4, and 10 min.) and observe the impact on the SWaT process over a period of 2 hours.

Impact. This attack essentially results in dropping of message m_2 shown in Figure 5, which delays the state transition $S_{11} \rightarrow S_{12}$ in $P1$. As a result, $P1$ remains at State S_{11} (idle state) even when $P2$ transitions to State S_{22} (ready state), and introduces operational delays. Figure 7 shows the

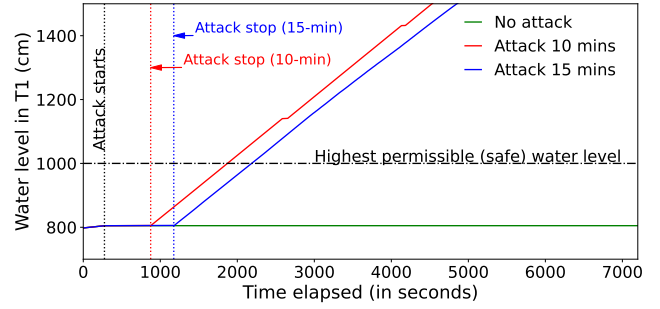


Figure 8: Impact of Tank Overflow Attack on the testbed.

impact of this delay on the level of purified water in the tank after 2 hours of operation. The water level effectively indicates the volume of water purified, since volume = water level \times tank cross-section and the cross-section is a constant. An attack lasting 2 min., 4 min., and 10 min. delays the state transition in $P1$ for 29s, 49s, and 81s, respectively, which in turn delays the filling up of the tank $T1$ by 6 min., 10.5 min., and 37 min., respectively, and reduces the output of $P6$ (i.e., volume of water purified) by 10.5%, 16%, and 37.7%, respectively. A reduction in the volume of purified water could cause inconvenience for customers, and financial losses for the company.

Tank Overflow Attack. In this attack, ICS-Sniper successfully dropped all the 30 packets of L_{12} during their 125th repetition. We execute this attack for three different packet drop durations (4, 10, and 15 min.), and observe the impact on the SWaT process over a period of 2 hours.

Impact. This attack essentially results in dropping of message m_3 shown in Figure 5, which delays the state transition $S_{12} \rightarrow S_{13}$ in $P1$. As a result, $P1$ remains in State S_{12} , while $P2$ transitions to State S_{23} .

Figure 8 shows the impact of delaying the transition by 10 and 15 min. on the water level in $T1$ for 2 hours of operation. We observed that a 4-min packet drop did not have any negative impact on $P1$, and hence we do not consider it. The water level in $T1$ begins to rise sharply as soon as ICS-Sniper completes the active attack phase and eventually goes past the highest permissible margin, i.e., 1000 cm. Effectively, $P1$ continues to fill tank $T1$ and pump water to $P2$, assuming $P2$ is going to consume the water, while in reality, $P2$ has closed its water inlet valve by then as $T2$ is full. This results in an overflow of $T1$, thereby causing an unsafe operating condition. Extending the packet drop duration beyond 10 min. does not change the impact of the attack, but only delays it.

Summary. The impact of both attacks on the process persists long after the active attack phase is over. The prolonged impact makes it challenging for the ICS administrators to identify the cause of the damages and take recovery actions. In general, the impact of both attacks increases proportionately with an increase in the duration of packet drops. However, dropping packets for arbitrary durations or dropping arbitrary packets could make the attack detectable.

Therefore, the adversary needs to strike a balance between attack impact and detectability (§6.3).

6.3. Detecting ICS-Sniper

Evaluation strategy. An effective detector would be able to detect attacks with high confidence and in a timely manner, regardless of the attack duration. We evaluate the efficacy of state-of-the-art detection techniques (§5.4) in detecting the attacks executed by ICS-Sniper in terms of detection efficacy and timeliness, as explained below.

Detection efficacy: We measure the efficacy of the detection techniques in terms of true positive rate (TPR) and false positive rate (FPR). For NND and Detano, we define TPR and FPR as follows:

$$\text{TPR} = \frac{\text{No. of windows where the detector correctly detected anomaly}}{\text{Total no. of windows in which ICS-Sniper dropped packets}}$$

$$\text{FPR} = \frac{\text{No. of windows where the detector incorrectly detected anomaly}}{\text{Total no. of windows in which ICS-Sniper did not drop packets}}$$

For PAD, the TPR and FPR are computed over the total number of sensor reading sets recorded in the system logs instead of windows. Over the entire evaluation period, the TPR and FPR of PAD are measured as follows.

$$\text{TPR} = \frac{\text{No. of log entries where PAD correctly detected anomaly}}{\text{No. of entries logged during the active attack phase}}$$

$$\text{FPR} = \frac{\text{No. of log entries where PAD incorrectly detected anomaly}}{\text{No. of entries logged when ICS-Sniper did not drop packets}}$$

An effective detector must have a high TPR and a low FPR. A low TPR would result in the detector missing the attack, while a high FPR would generate frequent false alarms, thereby increasing operational costs and delays.

Timeliness of detection: We use the attack detection delay as a measure of the detector’s timeliness, which is calculated as the difference between the time at which the detector raised a flag and the start time of the attack. Note that, window-based anomaly detectors, such as NND and Detano, treat an entire window-sized chunk of network traffic as a single data point for anomaly detection. Therefore, these techniques raise a flag only at time intervals that are multiples of the window size.

Experiment. We trained NND and Detano using the same encrypted traffic collected by ICS-Sniper for profiling sub-process $P1$. For evaluating the trained models, we collected $P1$ ’s network traffic during the active attack phase and replayed the traffic in the presence of the detectors. We varied the window sizes for both NND and Detano from 30 s to 30 min. to check if there exists an optimal window size that can detect any of the attacks of any duration in a timely manner. Prior to evaluating the detectors on the attack traffic, we also evaluated the base FPR of the techniques on a 2-hour-long traffic trace that was captured by running the SWaT process under non-adversarial conditions with

Detection Window Size (min.)	2-min drop				4-min drop				10-min drop			
	NND		Detano		NND		Detano		NND		Detano	
	TP (%)	FP (%)	TP (%)	FP (%)	TP (%)	FP (%)	TP (%)	FP (%)	TP (%)	FP (%)	TP (%)	FP (%)
0.5	0	9.7	0	10.1	0	8	12.5	14.1	0	5.4	0	34.2
1	0	2.5	0	8.6	0	8.5	25	8.9	0	7.5	0	30.7
2	0	9.6	0	1.4	0	11.1	0	9.5	10	15.7	0	28.1
5	0	16.7	0	7.1	0	16.7	0	0	10	7.7	0	23.1
10	100	28.6	0	0	100	15.4	0	0	50	15.4	0	15.4
30	100	40	0	0	0	20	0	0	100	30.8	0	0

TABLE 3: Efficacy of network traffic anomaly-based detectors in detecting Process Delay Attack

intermittent delaying and dropping of non-critical packets. We found the base FPR was 0 for both NND and Detano.

We trained PAD using the system logs from the same round of the SWaT process execution that was used for profiling sub-process $P1$. The SWaT process logged 30494 entries in the 8-hour operational cycle, with each entry containing 21 different sensor readings and process variables. PAD mined 19015 process invariants from the log. During the attack phase, the SWaT process logged \approx 4600 entries over 2 hours. We evaluated PAD on each of these entries.

Results. Table 3 shows the efficacy of network traffic anomaly-based detectors for different window sizes in detecting the Process Delay Attack for different durations of packet drops. We make four key observations from the experimental results. **(i)** Detano could detect the attack. It had a zero TPR for 2-min and 10-min attack durations for all window sizes, while its highest ever TPR was 25%, as seen in the case of the 4-min drop attack with a detection window size of 1-min. Even in this case, it incurred a high FPR of 8.9%. Since the number of windows with attacks (4) is far lesser than the number of benign windows (116), we consider 8.9% FPR to be a significant error. **(ii)** There was no instance where NND was able to detect all durations of the process delay attack with a 100% TPR. In cases where NND had a high TPR, it incurred a significantly high FPR as well, thereby making it unreliable. **(iii)** Even in cases where NND had a 100% TPR, it performed poorly in terms of timeliness of detection. For instance, we consider the case where NND had the highest TPR and lowest FPR, i.e., the 4-min attack for a window size of 10 min. In this case, the detection delay was 6 min. Our experimental results show that $P1$ had already suffered from a 4.5% reduction in the volume of treated water by then. **(iv)** PAD could not detect the attack at all (TPR=0), since the process variables did not violate any of the constraints, and the technique does not use time as a factor while mining invariants.

Table 4 shows the efficacy of network traffic anomaly-based detectors in detecting the Tank Overflow Attack for similar window sizes and packet drop durations of 10 min. and 15 min. Recall that in this attack, a 10-min packet drop is sufficient for causing safety violations. **(i)** While Detano has a zero TPR for most window sizes, the highest TPR (33%) was accompanied by a high FPR (11.9%). **(ii)** NND could detect an anomaly for 5-min and 10-min window sizes but incurred a high FPR in both cases. Furthermore, it also

Detection Window Size (min.)	10-min drop				15-min drop			
	NND		Detano		NND		Detano	
	TP (%)	FP (%)	TP (%)	FP (%)	TP (%)	FP (%)	TP (%)	FP (%)
0.5	0	6.6	33.3	11.9	0	6.2	35.5	31.3
1	0	6.6	18.2	8.1	0	16.7	37.5	24.6
2	0	13.1	0	9.5	0	13.8	37.5	24.6
5	100	13.2	0	0	100	15.4	50	16.7
10	100	12.5	0	0	100	23.0	50	8.3
30	0	16.6	0	0	100	20	0	0

TABLE 4: Efficacy of network traffic anomaly-based detectors in detecting Tank Overflow Attack

incurred a high detection delay: 5 min 28 s in case of the 5 min window, and 15 min 47 s in case of the 10-min window. By this time, the water level in $T1$ had reached a dangerous margin (900 cm). (iii) Comparing the performance of NND and Detano across two different packet drop durations, we can see that there was no single window size that could detect attacks of any duration in a consistent and timely manner. (iv) PAD detected an anomaly only when the water level in $T1$ had overflowed, which was too late.

Summary. For both attacks, the detection techniques either had a low TPR or had a high FPR along with a high TPR. The detection efficacy is heavily dependent on the window size configured (for NND, Detano), and it is challenging to set a window size that works well for all attacks, i.e., for all packet drop durations. Furthermore, even when they did detect the attack, the detection was too late.

7. Limitations and Countermeasures

7.1. Limitations of ICS-Sniper

ICS-Sniper has two main limitations. First, its efficacy depends on the differences in the inter-packet timings during the operational and idle phases of a batch-processing ICS. Continuous-processing ICSes do not have distinct operational and idle phases. Consequently, the differences in the inter-packet timings across different ICS states may not be drastic, which would make ICS-Sniper ineffective against such systems. However, many ICSes fall into the batch processing category, and hence ICS-Sniper is effective against them (§2.1).

Secondly, ICS-Sniper’s prototype currently handles only ICSes with a single PLC in each sub-process. In practice, ICSes may have more than one PLC in different sub-processes and inter-sub-process communication may involve communication between multiple PLCs across the sub-processes. Identifying critical messages in such a setup would require enhancing ICS-Sniper’s pattern mining algorithm. However, this extension should be straightforward.

7.2. Countermeasures

Traffic shaping. ICS-Sniper relies on correlations between packet metadata and the state transitions in the sub-processes. Therefore, a principled approach to mitigating the

attacks would require *shaping* the inter-sub-process traffic to break this correlation. A simple solution would be to ensure that all the messages transmitted in all states have the same size and are transmitted at fixed intervals. This approach could be implemented at the application layer or the network layer of the ICS, as we elaborate next.

Application layer shaping. Traffic shaping could be implemented in the application [14, 53]. The control logic could ensure that all messages in the inter-sub-process communication have the same payload size and are transmitted with a fixed inter-packet interval. However, changing the control logic potentially requires revisiting the entire ICS’s design to reason about the plant’s correctness, timeliness, and other safety conditions, which would incur non-trivial design and operational overheads.

In-network shaping. Alternatively, shaping could be implemented below the application layer in the network stack [32] or in the gateway router in each geolocation [33, 47]. To obfuscate packet sizes, a message could be padded with dummy bytes and a dummy header indicating the padding boundary, which could then be encrypted and encapsulated into a TCP packet. Obfuscating packet timings in ICSes, however, is challenging. Pacing the messages may delay the critical messages beyond tolerable thresholds, which would affect the operational safety of the ICS. Therefore, the network must inject dummy packets in the inter-sub-process traffic to achieve uniform inter-packet timing in each state. The bandwidth overhead due to dummy packets would depend on the diversity of message sizes and timings across all ICS states.

Redundancy in network paths. Shaping prevents an adversary from predicting critical messages, thus increasing the difficulty of performing a stealthy blackhole attack. To further improve resilience against attacks and network failures, ICSes could route their OT communication over multiple Internet paths to achieve redundancy. This could be implemented using source routing [11].

8. Conclusion

We present ICS-Sniper, a targeted blackhole attack on geo-distributed batch-processing ICSes. The periodic repetitive nature of the ICS communication and the correlation between packet sizes and ICS states makes it easy for an adversary to infer the underlying state-transition model of the ICS and identify the critical messages. Thus, ICS-Sniper can attack an ICS from outside the ICS perimeter—without any knowledge of the ICS’ internals—and cause significant damage by dropping only a few packets, thus evading detection. To ensure the operational safety of critical ICSes, strong mitigation techniques based on traffic shaping and redundancy in routing are required. We leave the design and evaluation of the mitigations to future work.

References

- [1] Marshall D. Abrams and Joe Weiss. Malicious Control System Cyber Security Attack Case

- Study: Maroochy Water Services, Australia. URL: <https://www.mitre.org/publications/technical-papers/malicious-control-system-cyber-security-attack-case-study-maroochy-water-services-australia>, Last accessed: Dec 6, 2023.
- [2] Acromag. Introduction to MODBUS TCP/IP. URL: https://www.prosoft-technology.com/kb/assets/intro_modbustcp.pdf, Last accessed: Dec 6, 2023.
 - [3] David Airehrour, Jairo Gutierrez, and Sayan Kumar Ray. Securing RPL routing protocol from blackhole attacks using a trust-based mechanism. In *International Telecommunication Networks and Applications Conference (ITNAC)*, pages 115–120. IEEE, 2016.
 - [4] Tejasvi Alladi, Vinay Chamola, and Sherali Zeadally. Industrial control systems: Cyberattack trends and countermeasures. *Computer Communications*, 155:1–8, 2020.
 - [5] Oxana Andreeva. Industrial Control Systems and their Online Availability. URL: https://media.kasperskycontenthub.com/wp-content/uploads/sites/43/2016/07/07190427/KL_REPORT_ICSAvailability_Statistics.pdf, Last accessed: Dec 6, 2023.
 - [6] Daniele Antonioli and Nils Ole Tippenhauer. MiniCPS: A toolkit for security research on CPS networks. In *ACM workshop on cyber-physical systems-security and/or privacy*, pages 91–100, 2015.
 - [7] Real Time Automation. An Introduction to MODBUS TCP/IP. URL: <https://www.rtautomation.com/technologies/modbus-tcpip/>, Last accessed: Dec 6, 2023.
 - [8] Real Time Automation. EtherNet/IP. URL: <https://www.rtautomation.com/technologies/ethernetip/>, Last accessed: Dec 6, 2023.
 - [9] Giovanni Barbieri, Mauro Conti, Nils Ole Tippenhauer, and Federico Turrin. Assessing the Use of Insecure ICS Protocols via IXP Network Traffic Analysis. In *International Conference on Computer Communications and Networks (ICCCN)*, pages 1–9. IEEE, 2021.
 - [10] Mike Barker and Jawahar Rawtani. *Practical batch process management*. Elsevier, 2004.
 - [11] David Barrera, Laurent Chuat, Adrian Perrig, Raphael M Reischuk, and Pawel Szalachowski. The SCION Internet Architecture. *Communications of the ACM*, 60(6), 2017.
 - [12] Kaspersky ICS CERT. Threat Landscape for Industrial Automation Systems. URL: <https://ics-cert.kaspersky.com/publications/reports/2023/03/06/threat-landscape-for-industrial-automation-systems-statistics-for-h2-2022/>, Last accessed: Dec 6, 2023.
 - [13] Yuqi Chen. SWaT Logic. URL: https://github.com/yuqiChen94/Swat_Simulator, Last accessed: Dec 6, 2023.
 - [14] Giovanni Cherubin, Jamie Hayes, and Marc Juarez. Website Fingerprinting Defenses at the Application Layer. In *Privacy Enhancing Technologies Symposium (PETS)*, 2017.
 - [15] M Herrero Collantes and A Lpez Padilla. Protocols and network security in ICS infrastructures. *Technology Report*, 2015.
 - [16] Rishabh Das, Vineetha Menon, and Thomas H Morris. On the edge realtime intrusion prevention system for DoS attack. In *International Symposium for ICS & SCADA Cyber Security Research*, pages 84–91, 2018.
 - [17] Dave Lundgren. Purdue 2.0: Exploring a New Model for IT/OT Management. URL: <https://www.redseal.net/purdue-2-0-exploring-a-new-model-for-it-ot-management/>, Last accessed: Dec 6, 2023.
 - [18] Davide Fauri, Bart de Wijs, Jerry den Hartog, Elisa Costante, Emmanuele Zambon, and Sandro Etalle. Encryption in ICS networks: A blessing or a curse? In *International Conference on Smart Grid Communications (SmartGridComm)*, pages 289–294. IEEE, 2017.
 - [19] Cheng Feng, Venkata Reddy Palleti, Aditya Mathur, and Deepthi Chana. A Systematic Framework to Generate Invariants for Anomaly Detection in Industrial Control Systems. In *NDSS*, 2019.
 - [20] Esther Galbrun, Peggy Cellier, Nikolaj Tatti, Alexandre Termier, and Bruno Crémilleux. Mining periodic patterns with a MDL criterion. In *Joint European Conference on Machine Learning and Knowledge Discovery in Databases*, pages 535–551. Springer, 2018.
 - [21] Oliver Gasser, Quirin Scheitle, Benedikt Rudolph, Carl Denis, Nadja Schricker, and Georg Carle. The amplification threat posed by publicly reachable BACnet devices. *Journal of Cyber Security and Mobility*, pages 77–104, 2017.
 - [22] Kwan Hee Han, Geon Lee, and Sang Hyun Choi. Manufacturing cycle time reduction for batch production in a shared worker environment. *International Journal of Production Research*, 51(1):1–8, 2013.
 - [23] IETF. The Transport Layer Security (TLS) Protocol Version 1.3. URL: <https://datatracker.ietf.org/doc/html/rfc8446>, Last accessed: Dec 6, 2023.
 - [24] SUTD iTrust. Secure Water Treatment (SWaT) Testbed, SUTD, Singapore. URL: https://itrust.sutd.edu.sg/itrust-labs-home/itrust-labs_swat/, Last accessed: Dec 6, 2023.
 - [25] Mayuri Khadpe, Pranita Binnar, and Faruk Kazi. Malware injection in operational technology networks. In *International Conference on Computing, Communication and Networking Technologies (ICCCNT)*, pages 1–6. IEEE, 2020.
 - [26] Marina Krotofil, Alvaro A Cárdenas, Bradley Manning, and Jason Larsen. CPS: Driving cyber-physical systems to unsafe operating conditions by timing DoS attacks on sensor signals. In *Computer Security Applications Conference*, pages 146–155, 2014.
 - [27] Chih-Yuan Lin and Simin Nadjm-Tehrani. Understanding IEC-60870-5-104 traffic patterns in SCADA networks. In *ACM Workshop on Cyber-Physical System Security*, pages 51–60, 2018.
 - [28] Loic Lefebvre. pyModbusTCP 0.2.0 . URL: <https://pypi.org/project/pyModbusTCP/>, Last accessed: Dec

- 6, 2023.
- [29] John Matherly. Shodan. URL: <https://www.shodan.io/>, Last accessed: Dec 6, 2023.
- [30] Aditya P Mathur and Nils Ole Tippenhauer. SWaT: A water treatment testbed for research and training on ICS security. In *International Workshop on Cyber-physical Systems for Smart Water Networks (CySWater)*, pages 31–36. IEEE, 2016.
- [31] Petr Matoušek, Vojtěch Havlena, and Lukáš Holík. Efficient modelling of ICS communication for anomaly detection using probabilistic automata. In *International Symposium on Integrated Network Management (IM)*, pages 81–89. IEEE, 2021.
- [32] Aastha Mehta, Mohamed Alzayat, Roberta De Viti, Björn B. Brandenburg, Peter Druschel, and Deepak Garg. Pacer: Comprehensive Network Side-Channel Mitigation in the Cloud. In *USENIX Security*, 2022.
- [33] Roland Meier, Vincent Lenders, and Laurent Vanbever. ditto: WAN Traffic Obfuscation at Line Rate. In *Network and Distributed System Security Symposium (NDSS)*, 2022.
- [34] Mininet. Mininet. URL: <http://mininet.org/>, Last accessed: Dec 6, 2023.
- [35] Mitre. Cisco DPC3928SL vulnerability. URL: <https://cve.mitre.org/cgi-bin/cvename.cgi?name=CVE-2017-5135>, Last accessed: Dec 6, 2023.
- [36] Mitre. Cisco IOS XE Software vulnerability, 2020. URL: <https://cve.mitre.org/cgi-bin/cvename.cgi?name=CVE-2020-3513>, Last accessed: Dec 6, 2023.
- [37] Mitre. Juniper Networks Junos OS vulnerability, 2023. URL: <https://cve.mitre.org/cgi-bin/cvename.cgi?name=CVE-2023-28983>, Last accessed: Dec 6, 2023.
- [38] Nizar Msadek, Ridha Soua, and Thomas Engel. Iot device fingerprinting: Machine learning based encrypted traffic analysis. In *Wireless Communications and Networking Conference (WCNC)*, pages 1–8. IEEE, 2019.
- [39] Gorby Kabasele Ndonga and Ramin Sadre. Exploiting the Temporal Behavior of State Transitions for Intrusion Detection in ICS/SCADA. *IEEE Access*, 10:111171–111187, 2022.
- [40] European Network and Information Security Agency. Protecting Industrial Control Systems. URL: <https://www.enisa.europa.eu/publications/protecting-industrial-control-systems.-recommendations-for-europe-and-member-states>, Last accessed: Dec 6, 2023.
- [41] Andrew Nicholson, Helge Janicke, and Antonio Cau. Position paper: Safety and security monitoring in ics/scada systems. In *Symposium for ICS & SCADA Cyber Security Research (ICS-CSR)*, pages 61–66, 2014.
- [42] Institute of Electrical and Electronic Engineers. EtherNet/IP: Industrial Protocol White Paper. URL: https://literature.rockwellautomation.com/idc/groups/literature/documents/wp/enet-wp001_-en-p.pdf, Last accessed: Dec 6, 2023.
- [43] Openvswitch.org. Open vSwitch Manual. URL: <https://www.openvswitch.org/support/dist-docs/ovs-ofctl.8.txt>, Last accessed: Dec 6, 2023.
- [44] Eva Papadogiannaki and Sotiris Ioannidis. A survey on encrypted network traffic analysis applications, techniques, and countermeasures. *ACM Computing Surveys (CSUR)*, 54(6):1–35, 2021.
- [45] Sandeep Gogineni Ravindrababu and Jim Alves-Foss. Analysis of Vulnerability Trends and Attacks in OT Systems. In *International Congress on Information and Communication Technology*, pages 127–142. Springer, 2022.
- [46] John S Rinaldi. EtherNet/IP and Transport Layer Security. URL: <https://www.rtautomation.com/rtas-blog/ethernet-ip-and-transport-layer-security/>, Last accessed: Dec 6, 2023.
- [47] Amir Sabzi, Rut Vora, Swati Goswami, Margo Seltzer, Mathias Lécuyer, and Aastha Mehta. NetShaper: A Differentially Private Network Side-Channel Mitigation System. In *USENIX Security*, 2024.
- [48] Takayuki Sasaki, Akira Fujita, Carlos H Ganán, Michel van Eeten, Katsunari Yoshioka, and Tsutomu Matsumoto. Exposed infrastructures: Discovery, attacks and remediation of insecure ics remote management devices. In *IEEE Symposium on Security and Privacy (SP)*, pages 2379–2396. IEEE, 2022.
- [49] Inc. Schneider Electric USA. Modbus/tcp security. URL: https://modbus.org/docs/MB-TCP-Security-v21_2018-07-24.pdf, Last accessed: Dec 6, 2023.
- [50] Sergiu Gatlan. Over 19,000 end-of-life Cisco routers exposed to RCE attacks. URL: <https://www.bleepingcomputer.com/news/security/over-19-000-end-of-life-cisco-routers-exposed-to-rce-attacks/>, Last accessed: Dec 6, 2023.
- [51] Jonathan Shorman and Steve Vockrodt. Ex-Employee Remotely Hacks Kansas Water Treatment Plant. URL: <https://www.governing.com/security/ex-employee-remotely-hacks-kansas-water-treatment-plant.html>, Last accessed: Dec 6, 2023.
- [52] Keith Stouffer, Victoria Pillitteri, Marshall Abrams, and Adam Hahn. Guide to Industrial Control Systems (ICS) Security. URL: <https://nvlpubs.nist.gov/nistpubs/SpecialPublications/NIST.SP.800-82r2.pdf>, Last accessed: Dec 6, 2023.
- [53] Tao Wang, Xiang Cai, Rishab Nithyanand, Rob Johnson, and Ian Goldberg. Effective attacks and provable defenses for website fingerprinting. In *USENIX Security*, pages 143–157, 2014.
- [54] Wireshark. tshark: Terminal-based Wireshark. URL: https://www.wireshark.org/docs/wsug_html_chunked/AppToolstshark.html, Last accessed: Dec 6, 2023.
- [55] Jeong-Han Yun, Yoonho Hwang, Woomyo Lee, Hee-Kap Ahn, and Sin-Kyu Kim. Statistical similarity of critical infrastructure network traffic based on nearest neighbor distances. In *Research in Attacks, Intrusions, and Defenses (RAID)*, 2018.

Appendix A. Pattern Mining Algorithm

Algorithm 1 shows the technique used by ICS-Sniper for mining patterns from encrypted traffic of the targeted sub-process while profiling it.

Appendix B. High-level Design of SWaT Testbed

Figure 9 shows the high-level design of the SWaT testbed that we used for our case study. We emulate six sub-processes: raw water storage (*P1*), chemical dosing (*P2*), ultrafiltration (*P3*), dechlorination (*P4*), reverse osmosis (*P5*), and backwash (*P6*). Each sub-process contains one PLC, which can communicate with every other sub-process via the Internet, which is emulated as a mesh network.

Figure 10 shows the components of the first two sub-processes of the SWaT test-bed, P1 and P2, in detail.

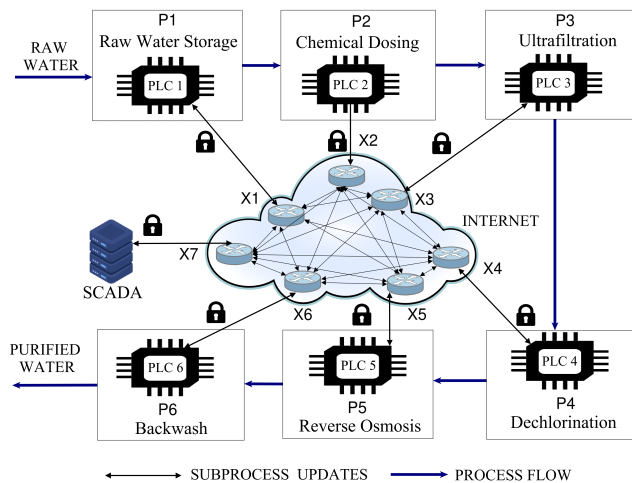


Figure 9: High-level design of the emulated SWaT test-bed. In our case study, we demonstrate a scenario where ICS-Sniper targets Sub-process P1.

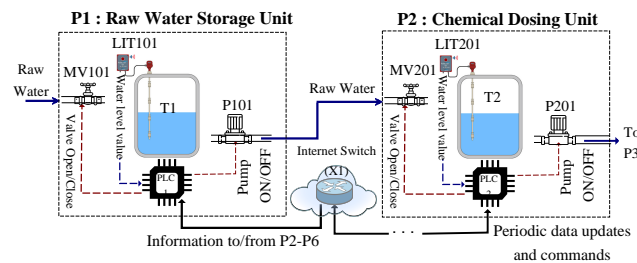


Figure 10: Sub-processes in our testbed targeted by ICS-Sniper. T1, T2: Water tanks; MV101, MV201: Water inlet valves; P101, P201: Pumps (outlet); LIT101, LIT201: Water level sensors.

Algorithm 1 Metadata pattern mining algorithm

Input : seq
Output : patterns[], repetitions[]

1: $patterns \leftarrow []$ ▷ Initializing global pattern set
2: $repetitions \leftarrow []$ ▷ Initializing a global set for storing the number of pattern repetitions

3: **procedure** FINDPATTERNS(seq, n) ▷ Procedure for finding patterns
4: $num_rep \leftarrow 1$ ▷ Initialization: Number of repetitions
5: **while** $length(seq) \geq 2n$ **do** ▷ Check if the sequence is long enough for a pattern of length n to repeat once
6: $first_n \leftarrow seq[:n]$ ▷ First sub-sequence of length n
7: $nextpos \leftarrow n$ ▷ Starting position of the sub-sequence to check for repetition of $first_n$
8: **while** $length(seq) \geq iter + 2n$ **do**
9: $next_n \leftarrow seq[iter : iter + n]$
10: **if** $first_n == next_n$ **then** ▷ Check if the first n elements repeat at least once
11: $patterns.append(first_n)$ ▷ Record the sub-sequence as a pattern if there is at least one repetition
12: $num_rep ++$
13: $nextpos \leftarrow nextpos + n$
14: **else** ▷ Pattern shift, or no repeating sub-sequence of length n found
15: **if** $num_rep > 1$ **then** ▷ Pattern shift
16: $repetitions.append(num_rep)$ ▷ Record number of pattern repetitions
17: $seq \leftarrow seq[n * num_rep :]$ ▷ Truncate the sequence
18: $n \leftarrow 0$ ▷ Re-initialize minimum sequence length
19: $num_rep = 1$ ▷ Re-initialize number of pattern repetitions
20: **end if**
21: $n \leftarrow n + 2$ ▷ Start from n=2 for pattern break, start from n=n+2 when no pattern of length n is found
22: **break**
23: **end if**
24: **end while**
25: **end while**
26: **return** seq ▷ Return the elements left in the sequence after extracting patterns
27: **end procedure**

28: $residuals \leftarrow FINDPATTERNS(seq, 2)$ ▷ Start with finding patterns of the shortest length in input metadata sequence
29:
30: **while** $residuals \neq NULL$ **do** ▷ There are residual elements after extracting some patterns
31: $seq \leftarrow (patterns[-1]).concat(residuals)$ ▷ Add back one round of repetition of the last extracted pattern at the beginning of truncated sequence
32: $patlen \leftarrow length(patterns[-1])$ ▷ Length of last extracted pattern
33: $repetitions[-1] \leftarrow repetitions[-1] - 1$
34: **if** $repetitions[-1] == 0$ **then**
35: $patterns \leftarrow pattern[: -1]$
36: $repetitions \leftarrow repetitions[: -1]$
37: **end if**
38: $residuals \leftarrow FINDPATTERNS(seq, patlen + 2)$ ▷ Try to find patterns that are longer than the last extracted pattern
39: **end while** ▷ Continue until there is no residual element
40: **return** $patterns, repetitions$
